Catalysis Today 158 (2010) 317–323

Contents lists available at ScienceDirect

Catalysis Today

journal homepage: www.elsevier.com/locate/cattod

Hydrogen adsorption on NiNaY composites at room and cryogenic temperatures

Ronggang Ding[a], Zhonghua Zhu[a], Xiangdong Yao[a], Zifeng Yan[b], Gaoqing Max Lu[a,*]

[a] ARC Centre of Excellence for Functional Nanomaterials, University of Queensland, Brisbane, Qld 4072, Australia
[b] College of Chemistry and Chemical Engineering, China University of Petroleum, Qingdao, China

ARTICLE INFO

Article history:
Available online 28 April 2010

Keywords:
Hydrogen spillover
NiNaY composite
Dissociative hydrogen adsorption

ABSTRACT

The NiNaY composites have been investigated using various techniques to explore their hydrogen adsorption performance and structural characteristics. Hydrogen adsorption capacities of reduced NiNaY composites were significantly enhanced under various temperatures and pressures. Most noteworthy is that at room temperature and low pressure, hydrogen adsorption amount was increased by a remarkable factor of 7.1 for reduced 10 wt% NiNaY composite. Dissociative hydrogen adsorption and subsequent hydrogen spillover at high pressure have enhanced hydrogen adsorption capacity by a factor of 0.4 and 0.86 on reduced 10 wt% NiNaY composite at 77 and 303 K, respectively. The enhancement effect of hydrogen adsorption on the reduced composites at room temperature is determined by hydrogen adsorption on available nickel sites which were characterized by the active nickel surface areas. However, the optimized hydrogen adsorption enhancement effect on the composite at 77 K is achieved by a combination of suitable active nickel surface area and active support area. The results suggest that spillover effect is occurring at 77 K on the reduced NiNaY composites.

1. Introduction

It is well known that considerable controversy exists in the large amounts of hydrogen storage in various carbon nanomaterials. Nonetheless, one common feature existed in the reported experiments on hydrogen storage in carbon nanomaterials: irreversibly adsorbed species and the presence of reduced transition nickels. In the late 1980s, Schwarz pioneered the concept of adding small amounts of transition metals to activated carbons in order to increase their storage capacity through the hydrogen spillover mechanism [1,2]. A so-called metal-assisted cold storage (MACS) technique was proposed to enhance the hydrogen adsorption on Pd- and Pt-assisted carbon materials via hydrogen spillover. The cryogenic hydrogen storage was significantly enhanced due to the addition of 5 wt% Pd on an activated carbon with surface area of 1167 m^2/g, from 4.9 wt% to 7.0 wt% at 4 MPa and 77 K [1,2]. The hydrogen spillover effect has long been observed over supported metal catalysts, which is described as the dissociative chemisorption of hydrogen on the catalyst metal particles and followed by migration of atomic hydrogen onto the surface of the support [3]. Hydrogen spillover can be assessed in a number of ways, but perhaps the most common is simple calculation of the hydrogen to nickel ratio, either the surface nickel (M_S) or total nickel (M_T) content. When spillover occurs, the H:M_S will typically exceed unity; in the case of materials that form hydrides, the H:M_T will exceed the stoichiometric ratio of the hydride [4].

Later, Yang et al. proposed a spillover-enhanced mechanism for improved hydrogen storage in multiwalled carbon nanotubes involving hydrogen dissociation on nickel particles followed by atomic hydrogen spillover and adsorption on the nanostructured carbon surface [5]. Since then, Yang's group has explored the hydrogen spillover effect at room temperature on various adsorbents, including activated carbons, zeolites, metal organic frameworks (MOFs), covalent organic frameworks (COFs) and other nanostructured materials, and attributed the significant hydrogen adsorption enhancement to the secondary spillover and carbon bridge establishment strategy [6–13]. By building carbon bridges, the hydrogen uptake increased from 0.5 wt% on pure IRMOF-8 to 4 wt% on bridged IRMOF-8 at 10 MPa and 298 K [9]. From kinetic point of view, doping with VCl_3 and TCl_3 effectively increased the rates of adsorption and desorption by spillover and also decreased the heats of adsorption and activation energies for spillover [10]. A comprehensive review of the subject has been published in 2008 by Wang and Yang [14].

Numerous other examples of enhanced hydrogen uptake in presence of transition metals have also been reported recently and explained by spillover mechanism [15–24]. Ni supported on activated carbon and nanospheres and Ni-plated carbon nanofibers exhibited the hydrogen adsorption enhancement by the spillover from Ni particles to the support surfaces [17,21,22]. Spoto et al. have explored the possibility to use the spillover effect to favor the diffusion of hydrogen in all the available voids of a zeolitic framework at room temperature. It was found that atomic hydrogen

* Corresponding author. Tel.: +61 7 3365 9044; fax: +61 7 3365 9040.
E-mail address: m.lu@uq.edu.au (G.M. Lu).

0920-5861/$ – see front matter.
doi:10.1016/j.cattod.2010.04.002

can penetrate the hexagonal openings of the Pd-containing zeolite framework (calculated barrier of 16 kJ/mol) and diffuse into the sodalite cages, as predicted by the ab initio calculations. The very fast exchange rate observed at room temperature suggests the occurrence of some factors responsible for the lowering of the diffusional barrier [19].

Very recently, the formation of the atomic hydrogen in presence of a Pd-modified activated carbon fiber and their subsequent spillover and binding to the carbon support at room temperature has been confirmed by inelastic neutron scattering (INS) [16]. However, the possible hydrogen spillover effect and enhanced hydrogen adsorption at cryogenic temperature have not been explored yet. After Schwarz's pioneering work on Pd-assisted carbon under the temperature range from 77 to 373 K, little research has been done on spillover-enhanced hydrogen adsorption at cryogenic temperatures. Although nickel–zeolite was also mentioned by Schwarz as a potential hydrogen adsorption material, experimental verification of enhanced hydrogen adsorption on this material was not conducted [1]. A study of characterization of Ru–Cu catalysts using H_2 chemisorption confirmed that hydrogen chemisorbs on the studied metal catalyst at 77 K, however, the existence of Cu suppressed the hydrogen spillover on Ru metal particles [25].

In this article, a series of NiNaY composites prepared using traditional impregnation method have been studied for spillover-enhanced hydrogen adsorption at both room and cryogenic temperatures. The hydrogen spillover effect was investigated in detail and hydrogen adsorption enhancement was quantitatively determined, confirming the occurrence of hydrogen dissociation and spillover at cryogenic temperatures. The objective of this work is to better understand how hydrogen spillover affects storage rather than serve as an ultimate media for practical hydrogen storage.

2. Experimental

2.1. Synthesis of NiNaY composites

A series of NiNaY composites were synthesized by incipient wetness impregnation method. The NaY zeolite (Sigma–Aldrich Chemical) was calcined at 773 K for at least 4 h to remove the moisture and other impurities. Nickel nitrate solutions were prepared according to the calculated nickel loadings (1, 5, 10 and 20 wt%). Then the calcined zeolite was impregnated in nickel nitrate solution overnight, followed by drying at 383 K for 12 h and then calcination at 773 K in air for 6 h. The reduced NiNaY composite materials were obtained by reduction at 773 K in the H_2 flow for 2 h.

2.2. N_2 adsorption

N_2 adsorption/desorption isotherms of the samples at 77 K were obtained using Autosorb-1 (Quantachrome Instruments, USA) gas sorption analyzer. Samples were usually degassed at 473 K for 10 h prior to the adsorption analysis. The surface area, S_{BET}, was calculated by BET equation usually in the relative pressure range of 0.05–0.25. Total pore volume (V_t) was determined at $P/P_0 = 0.995$. The micropore surface area, S_{micro}, and pore volume (V_{micro}) were calculated by the *t*-plot method. The mesopore surface area (S_{meso}) and volume (V_{meso}) were derived by subtracting the S_{micro} and V_{micro} from the S_{BET} and V_t, respectively.

2.3. H_2 chemisorption

The metal surface areas (S_m, in m^2/g), metal dispersions (D, in %), and metal particle sizes (d, in nm) of the reduced NiNaY composites were determined by H_2 chemisorption on a Quantachrome Autosorb-1 analyzer. The samples were heated in flowing He at 373 K for 30 min and then the temperature was increased to designated reduction temperature (773 K). At this temperature, the helium flow was switched to hydrogen flow and the samples were reduced for 2 h and subsequently degassed for 30 min, and finally cooled to 303 K for hydrogen adsorption. The monolayer gas uptake was obtained by extrapolating to zero pressure the linear portion of the isotherm above the saturation pressure.

2.4. Hydrogen adsorption capacity measurement

Hydrogen adsorption isotherms at low pressure up to 0.1 MPa were obtained on the Autosorb-1 analyzer. The measurement temperature ranged from 77 to 303 K. The samples were degassed at 473 K for 10 h prior to the adsorption analysis. Hydrogen adsorption measurements on Autosorb-1 at low pressure range provide excellent accuracy of adsorption capacities due to the high-resolution measurements of pressures and temperatures. The repeated measurements on Autosorb-1 analyzer up to 0.1 MPa exhibited excellent resolution and reproducibility with negligible standard error.

A commercial rig made by Japanese company Suzuki-Shaokan was used to measure the hydrogen adsorption capacity at high pressures based on the volumetric analysis technique. Every set of hydrogen adsorption tests involved the blank tests and actual hydrogen adsorption capacity measurements. Both blank tests and actual measurements involved two measurements at two different temperatures, i.e., room temperature and 77 K. Blank tests at room temperature measured the total volume (sum of the sample cylinder and the gas line volume), while blank tests at 77 K determined the distribution of the sample cylinder volume (cold zone) and the line volume (warm zone). The volume of sample cylinder depends on the level of cylinder immersed into the liquid nitrogen. For blank test and the corresponding hydrogen adsorption test at 77 K, the sample cylinder was always positioned at the same liquid nitrogen level so that the measurement conditions remained the same. The result of blank tests was expressed as a deviation from zero line, which will be subtracted as a background from the actual hydrogen tests. Thus the system error of the test was minimized and reliable data can be obtained. The hydrogen adsorption capacities under high pressures were measured three times and the standard error was estimated within 0.3–0.8%. The error bar was not shown in the figures for clear view where multicurves were next to each other.

3. Results and discussion

3.1. Textural property of NiNaY composites

The textural properties of calcined NaY zeolite, calcined NiNaY composites and reduced NiNaY composites measured by N_2 adsorption are shown in Table 1. According to the data shown in Table 1, the impregnation resulted in the decrease of the surface areas and pore volumes of the NaY supports. Both micropore and mesopore surface areas decreased with the increased nickel loading. It indicated that nickel ions not only deposit on the micropore surface but also on the mesopore surface. However, the greater reduction of micropore volumes and surface areas with increased Ni loading indicated that most nickel ions enter and deposit in the micropores.

The reduction process resulted in further decrease of the surface areas and pore volumes of the composites. It was believed that nickel ions can migrate to small pores or cavities within the framework of NaY zeolite support under the reduction conditions. Occupation of the small pores of the zeolite resulted in the further decrease of the micropore volume and surface areas.

Table 1
Textural properties of NaY, calcined NiNaY and reduced NiNaY composites.

Sample	S_{BET} (m^2/g)	V_t (cm^3/g)	V_{mic} (cm^3/g)	S_{mic} (cm^3/g)	S_{meso} (m^2/g)
NaY	887	0.375	0.335	760	127
1%NiNaY	863	0.362	0.277	738	125
Reduced 1%NiNaY	853	0.358	0.274	730	123
5%NiNaY	802	0.343	0.261	702	100
Reduced 5%NiNaY	779	0.336	0.254	675	104
10%NiNaY	762	0.317	0.248	666	96
Reduced 10%NiNaY	732	0.306	0.239	634	98
20%NiNaY	553	0.246	0.174	461	92
Reduced 20%NiNaY	542	0.236	0.161	445	97

In the meantime, the mesopore surface areas of the composites remained nearly unchanged after hydrogen reduction. It seemed that the nickel ions migrate from mesopores to micropores during reduction process. This re-dispersion of the nickel particles during reduction process is beneficial to the hydrogen adsorption which will be discussed below.

3.2. Hydrogen adsorption on NiNaY composites

Hydrogen adsorption performance of reduced NiNaY composites was evaluated at various pressures and temperatures. Fig. 1 shows the hydrogen excess adsorption isotherms at 77 K and high pressure for reduced NiNaY composites. The appearance of maximum point is a feature of excess adsorption under supercritical conditions although the maximum point is usually not achieved yet in the testing pressure range at much higher temperatures above the critical temperature of the adsorbate. The excess adsorption is defined as the difference between the amount of hydrogen stored on the surface of an adsorbent at a certain temperature and pressure and the amount that would be present in the porous material under the same conditions in the absence of surface–gas interactions. Due to the inherent feature of adsorption, the experimentally measured adsorption amount is actually excess adsorption instead of so-called absolute adsorption.

The relationship between the measured excess amount of adsorption and the absolute adsorption is described by the Gibbs definition of adsorption [26]:

$$n = n_{abs} - \rho_g V_a = V_a\rho_a - V_a\rho_g = V_a(\rho_a - \rho_g) \quad (1)$$

where ρ_a is the density of the adsorbed phase, ρ_g is the density of the gas phase, and V_a is the volume of the adsorbed phase. Eq. (1) clearly shows that n is a density excess amount, while n_{abs} is the total mass confined in the adsorbed phase and named as absolute adsorption. $V_a\rho_g$ is usually negligible at subcritical temperatures due to very small gas phase density depending on the saturated vapour pressure, thus excess adsorption approximately equals to absolute adsorption. However, it becomes very large under supercritical conditions since gas density rises dramatically with pressure.

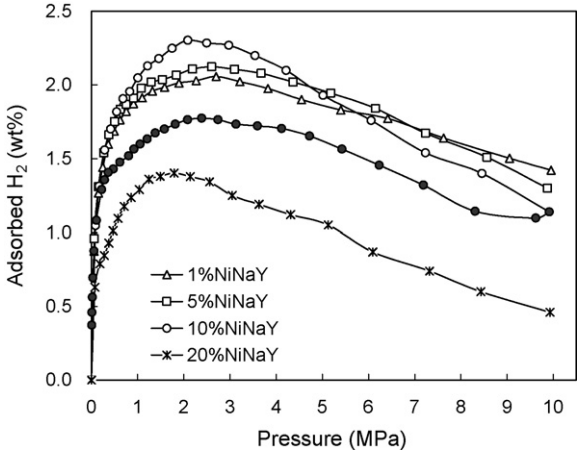

Fig. 1. Hydrogen excess adsorption isotherms on the reduced NiNaY composites at 77 K and high pressure. Solid circle: desorption isotherm for 10% NiNaY composite.

The appearance of maximum in the hydrogen adsorption isotherms at 77 K and high pressures (Fig. 1) can be explained as follows. Density of adsorbed hydrogen (ρ_a) increases with the gas pressure, so does the density of the compressed hydrogen gas (ρ_g). ρ_a is a function of adsorption energy distribution of solid surface and gas pressure, while ρ_g is a function of only gas pressure. Increase of ρ_a is limited by the number of adsorption sites of solid surface, but increase of ρ_g is limitless in the tested pressure range. Therefore, the difference between the two phase density ($\rho_a - \rho_g$) becomes smaller and smaller with increased adsorption pressure, until the appearance of isotherm maximum. At this maximum point, ρ_g equals to ρ_a. The excess adsorption capacity will decrease with the continuously increased pressure beyond the maximum point. The presence of a maximum in the isotherms at high pressure and low temperature is a typical feature of excess adsorption isotherms under supercritical conditions. It occurs when the density of the coexistent bulk gas phase increases faster than the adsorbed phase [27]. Depending on the adsorption conditions and tested material, the pressure range of appearance of the maximum will vary accordingly.

The hydrogen uptakes of the composites were found to increase with increased nickel loading. However, hydrogen uptake increased only up to a Ni loading of 10 wt%. 20 wt% NiNaY composite underwent a dramatic decrease of hydrogen uptake. This phenomenon can be ascribed to the textual structure changes of the composites and spillover effect which are discussed in detail in the following section.

Desorption branch of only one composite (10%NiNaY) at 77 K and high pressure is also shown in Fig. 1. Other three composites possessed the similar desorption branches which are not shown here for clear view. Adsorbed hydrogen on 10%NiNaY composite was not fully desorbed. At low pressure of 0.03 MPa and 77 K, there was still 0.3 wt% of hydrogen remaining on the adsorbent which can be fully desorbed at higher temperature. It is believed that the trapped hydrogen is from the dissociated and spiltover hydrogen in the presence of Ni nanoparticles. The trapped hydrogen atoms, possibly inside the small cavities (e.g. sodalite cages), cannot be released at 77 K and can only be released at higher temperatures.

The hydrogen excess adsorption isotherms of reduced NiNaY composites at room temperature generally followed a linear trend with the pressure (Fig. 2). The effect of nickel loading on the hydrogen adsorption at room temperature demonstrated the same trend as that at 77 K, i.e., 20% NiNaY composite showed a significant decrease of hydrogen adsorption while other three composites showed enhanced hydrogen uptakes with elevated nickel loadings.

The desorption behavior of the reduced composites at room temperature is different from that at 77 K. For the clear view, only one desorption branch for 10% NiNaY is shown in the figure. As shown in Fig. 2, a hysteresis appeared although adsorbed hydro-

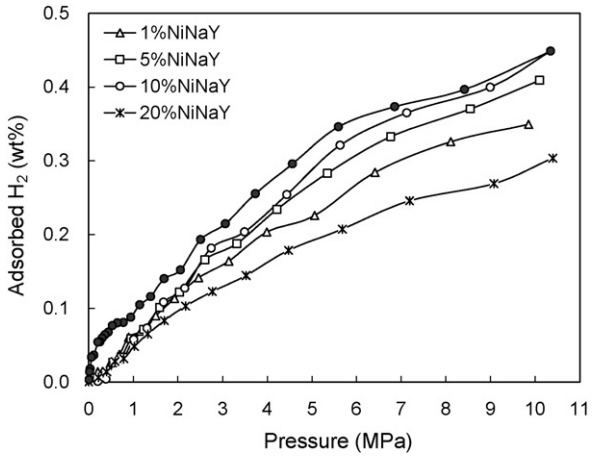

Fig. 2. Hydrogen excess adsorption isotherms on the reduced NiNaY composites at 295 K and high pressure. Solid circle: desorption isotherm for 10% NiNaY composite.

gen was fully desorbed. On the calcined composite, the adsorption and desorption isotherms were fully reversible without hysteresis (not shown). The hysteresis on the reduced composite is believed to originate from desorption of recombined hydrogen atoms which adsorbed on nickel particles, dissociated and diffused into the surface of the support. Recent studies showed that desorption process follow a reverse spillover process after enhanced adsorption by hydrogen spillover [11,28,29]. Reverse spillover is when a spiltover species diffuses back to and moves onto the source of spillover. Reverse spillover assumes that the species under consideration cannot adsorb directly on the acceptor surface and only gets there by spillover [3]. In this case, the spiltover hydrogen atoms dispersed in NaY zeolite pores diffuse back to Ni nanoparticles and recombine to hydrogen molecule and desorb.

Fig. 3 shows hydrogen excess adsorption isotherms on the reduced NiNaY composites at 77 K and up to 0.1 MPa. Hydrogen adsorption capacities of NaY, NiNaY composites and reduced NiNaY composites under various pressures and temperatures are shown in Table 2. Hydrogen adsorption on reduced composites was greatly enhanced and the corresponding enhancement factors are also listed in Table 2. The hydrogen adsorption capacities of calcined NiNaY composites continuously decreased with increased nickel loading at various temperatures and pressures. This trend was not that clear for hydrogen adsorption at 303 K and low pressure due

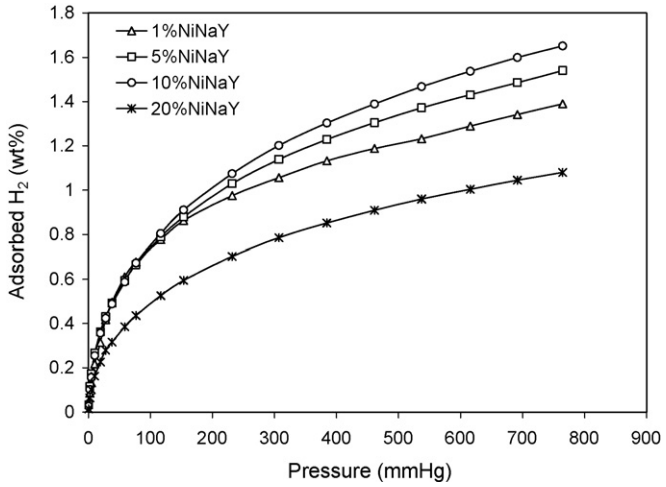

Fig. 3. Hydrogen excess adsorption isotherms on the reduced NiNaY composites at 77 K and up to 0.1 MPa.

to generally very low hydrogen uptake. It is reasonable because NiNaY composites have reduced surface areas and micropore volumes with increased nickel loading. The nickel particles exist in the form of NiO in the calcined NiNaY composites and impossible to provide chemisorption sites for hydrogen.

For reduced NiNaY composites, it is a different story. Hydrogen adsorption capacities of reduced composites were significantly enhanced under various temperatures and pressures. Most noteworthy is that hydrogen adsorption capacity on reduced 10% NiNaY reached 1.65 wt% at 0.1 MPa and 77 K, compared with a 1.01 wt% of adsorbed hydrogen on calcined 10% NiNaY. It was also marked with a hydrogen uptake enhancement from 0.241 to 0.449 wt% on the same composite after reduction at high pressure and room temperature, with an enhancement factor of 0.86. On the reduced 10%NiNaY composite, hydrogen adsorption capacity increased from 1.64 to 2.30 wt% at high pressure and 77 K, a 40% improvement compared with the calcined 10% NiNaY composite.

At room temperature and low pressure, hydrogen adsorption amount was increased by a remarkable factor of 7.1 for reduced 10% NiNaY composite. Although the hydrogen adsorption capacity is very low under these conditions, this dramatic enhancement implies a promising medium to store large amount of hydrogen when the combination of pressure and temperature becomes suitable. As was evident from the data shown in Tables 1 and 2, the micropore volume and surface area of reduced composites slightly decreased after reduction, but their hydrogen uptakes were greatly improved. It seemed that reduced nickel particles play an important role in enhancing hydrogen adsorption capacities on the reduced NiNaY composites.

It is also noteworthy that the enhancement effect was more obvious at low pressure and room temperature. At low pressure and room temperature, the adsorbed hydrogen on reduced NiNaY composites was dilute and thus more sites are accessible to spiltover hydrogen. At low temperature and high pressure, the adsorbed hydrogen on reduced NiNaY composites was much denser and less sites were available for spiltover hydrogen thus enhancement effect due to spillover was limited.

3.3. Spillover effect on composites

In order to elucidate the influence of Ni loading and Ni particle size on the enhancement of hydrogen adsorption, the reduced NiNaY composites were investigated using H_2 chemisorption. Generally, XRD, TEM and gas chemisorption can be employed to estimate the size of nickel particles distributed over the surface of the support. XRD is a relatively unreliable, inaccurate method of estimating average crystallite diameter, especially for low nickel loading and small particle size [30]. TEM provides direct measurement of crystallite size with more information, such as particle shape and texture, but it is time consuming to estimate the average crystallite size. The average crystallite size is usually determined on the basis of the dispersion (fraction of nickel atoms exposed) measured by hydrogen or CO chemisorption. H_2 chemisorption is a convenient, accurate and generally applicable technique for estimating surface content and average crystallite size of supported nickel [30].

The amount of nickel on the surface, M_S, was estimated by the hydrogen chemisorption isotherm extrapolation method introduced by Benson and Boudart [31] in which the hydrogen isotherm from low pressures (0.007–0.03 MPa) is extrapolated to zero pressure to determine the monolayer surface coverage of the catalyst:

$$N_M = \lim_{P \to 0} N_T$$

Table 2
Hydrogen adsorption capacities of NaY, calcined NiNaY and reduced NiNaY composites and the enhancement factors under various pressures and temperatures.

Sample	Adsorbed H_2 (wt%) Low P (0.1 MPa)				Adsorbed H_2 (wt%) High P (10 MPa[a])			
	77 K	EF	303 K	EF	77 K	EF	295 K	EF
NaY	1.10		0.008		1.85		0.28	
1%NiNaY	1.03		0.008		1.79		0.271	
Reduced 1%NiNaY	1.39	0.35	0.020	1.5	2.06	0.16	0.349	0.29
5%NiNaY	1.02		0.007		1.73		0.26	
Reduced 5%NiNaY	1.54	0.51	0.04	4.7	2.12	0.23	0.409	0.57
10%NiNaY	1.01		0.007		1.64		0.241	
Reduced 10%NiNaY	1.65	0.63	0.057	7.1	2.30	0.4	0.449	0.86
20%NiNaY	0.91		0.006		1.29		0.217	
Reduced 20%NiNaY	1.08	0.19	0.030	4.0	1.40	0.09	0.304	0.4

EF: enhancement factor of reduced NiNaY composite due to spillover, compared with calcined NiNaY composite with the same nickel loading.
[a] The pressure range is 0–10 MPa for 77 and 295 K tests. At 77 K, hydrogen adsorption data listed in the table were the maximum values taken at certain pressures depending on the samples.

where N_M is the monolayer uptake by the nickel, N_T is the total hydrogen uptake of the material, including both the nickel and support adsorbent. This extrapolated value was then used to calculate the atoms of nickel on the surface per gram of material, assuming that each surface nickel atom interacted with one hydrogen atom (e.g. $H/M_S = 1$). This value of M_S was then used in calculation of nickel dispersion, by comparing to the nickel content.

Fig. 4 showed hydrogen uptakes on the reduced NiNaY composites at 303 K and up to 0.1 MPa for nickel dispersion determination. The hydrogen adsorption capacities of the reduced NiNaY composites were listed in Table 2. The calculated nickel dispersions, crystallite sizes, active surface areas and hydrogen uptakes of reduced NiNaY composites were shown in Table 3.

It was evident that nickel dispersion of the composites decreased with increased nickel loading. This is reasonable because less nickel better disperses on the surface of the support. Correspondingly, the average crystallite size increased from 1.6 to 13.4 nm with increased nickel loading. Boudart [32] classified supported nickels into three categories according to particle size, as follows: (a) nickel particles larger than about 5 nm, which have surface structures resembling those of chunks of the bulk nickel; (b) supported nickel particles in the size range 1–5 nm which have most interesting catalytic properties; (c) supported nickel particles with diameters below 1 nm, which are referred to as clusters. In this study, particle size of three composites with nickel loading less than 10 wt% fall within 1–5 nm category, while the highest nickel loading of 20 wt% form the biggest nickel particle with the size of 13.4 nm.

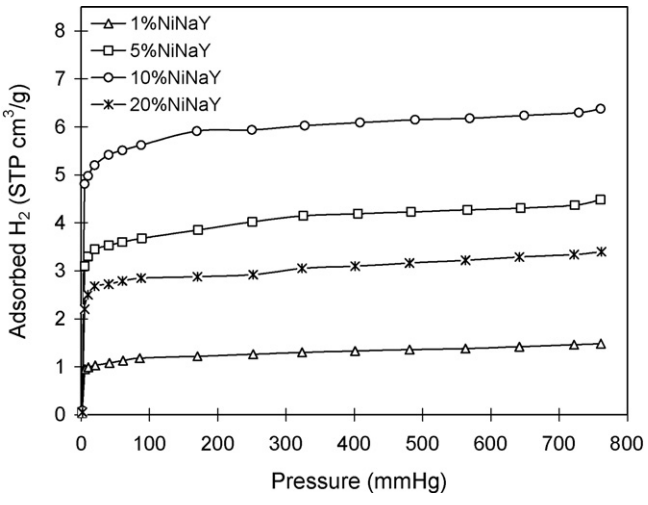

Fig. 4. Hydrogen excess adsorption isotherms on the reduced NiNaY composites at 303 K and up to 0.1 MPa.

The smaller the nickel particles, the larger the fraction of the nickel atoms that are exposed at surfaces, where they are accessible to hydrogen molecules for dissociative adsorption.

The comparison of Tables 2 and 3 suggests that active nickel surface area plays a key role in hydrogen adsorption enhancement at room temperature. Actually, enhancement factor at room temperature was proportionally related to active nickel surface area of reduced NiNaY composites. The enhancement was a comprehensive effect of hydrogen adsorption on nickel nanoparticles and hydrogen spillover into available adsorption sites on zeolite support (active support surface area). The hydrogen adsorption was dilute at room temperature and active support surface area was not a limiting factor. Rather, the enhancement effect of hydrogen adsorption on the reduced composites at room temperature was determined by hydrogen adsorption on available nickel sites which were characterized by the active nickel surface areas.

However, dense hydrogen adsorption at 77 K greatly reduced the active support surface area and the ultimate enhancement effect was significantly restricted by the active support surface area. Although the surface area of the composite was not the same as the active support surface area, its change implied the change of active support area. When the nickel loading increased from 10 to 20 wt%, the corresponding surface areas of reduced composites decreased from 732 to 542 m^2/g. This decrease was responsible for the dramatic reduction of enhancement factors for 20% NiNaY composite at 77 K (Enhancement factors are 0.19 and 0.09, respectively, at 0.1 MPa and high pressure). It seemed that optimized hydrogen adsorption enhancement effect on the reduced NiNaY composite at 77 K is achieved by a combination of suitable active nickel surface area and active support area.

The inclusion of a small amount of nickel led to a significant increase of the amount of hydrogen that can be stored on NaY zeolite alone. The amount of stored hydrogen increase far exceeded the amount that would be expected due to sorption on nickel. When the gaseous hydrogen was brought into contact with active nickel, hydrogen molecules were adsorbed onto the surface of nickel, and some of these molecules were dissociated into hydrogen atoms. When the nickel was dispersed as small particles on a high surface area support matrix such as NaY zeolite, the monatomic hydrogen species spilt onto nearby sites on the support matrix, and became adsorbed thereon. The activated form of hydrogen thus produced is more efficient at filling the available sites on the zeolite. A typical NaY zeolite (faujasite type) unit cell formula is $Na_j[(AlO_2)_j(SiO_2)_{192-j}]\cdot zH_2O$, where the Na cations are exchange ions compensating the negative charge of the framework (one per Al atom). NaY zeolite has three-dimensional pore structures incorporating nearly spherical cages with diameters of about 1.2 nm connected by apertures that are 12-membered oxygen rings, with diameters of about 0.75 nm [33]. The small cages, such as β and

Table 3
Hydrogen monolayer uptakes, active surface areas, nickel dispersions and crystallite sizes of the reduced NiNaY composites.

Sample	Monolayer uptake (μmol/g)	Active surface area (m^2/g)	Nickel Dispersion (%)	Crystallite size (nm)
Reduced 1%NiNaY	55.0	4.3	64.6	1.6
Reduced 5%NiNaY	154.0	12.0	36.2	2.8
Reduced 10%NiNaY	235.0	18.4	27.6	3.7
Reduced 20%NiNaY	129.0	10.1	7.6	13.4

Table 4
Hydrogen spillover results of reduced NiNaY composites under different adsorption conditions.

Ni content (wt%)	$H:M_S$			
	303 K and 0.1 MPa	295 K and 10 MPa	77 K and 0.1 MPa	77 K and high P[a]
1%	1.05	7.1	32.7	24.6
5%	1.14	4.9	16.9	12.7
10%	1.27	4.4	13.6	14.0
20%	1.07	3.4	6.6	8.1

[a] Data listed in the table were the maximum values taken at certain pressures depending on the samples.

sodalite cages, have the window sizes of 0.22–0.24 nm that are 6-membered oxygen rings. Hydrogen molecule has a kinetic diameter of 0.289 nm and impossible to enter these small cages and be trapped there. However, the dissociated monatomic hydrogen, with the diameter around 0.1 nm, is quite easy to access these small adsorption sites.

Spoto et al. suggested that the transit of a hydrogen atom through a silicate ring is only one of the possible mechanisms for hydrogen transport to and from the sodalite-cages. In fact, it is well known that the protons eventually present on the ring migrate to neighbouring rings, thus contributing to the mobility of hydrogen atoms in the silicate framework [19]. These considerations suggested that the presence inside the NaY zeolite of additional catalytic centres able to split the H_2 molecule (like Ni metal nano-clusters) could strongly improve the penetration probability of hydrogen inside the sodalite-cage and the hexagonal prism. The change of micropore and mesopore volumes before and after reduction on NiNaY composites indicated that nickel ions can migrate to small pores or cavities within the framework of NaY zeolite support under the reduction conditions (see Section 3.1). These findings offer a reasonable explanation of the significant hydrogen adsorption enhancement on the reduced NiNaY composites.

The amount of spiltover H_2 generally should be the difference between H_2 adsorption capacities of undoped support and the reduced metal/support adsorbent. Although this principle applies to hydrogen spillover-enhanced adsorption well at most cases as shown in the precious literature [6,15], which mainly considered hydrogen adsorption above room temperature, it does not apply to the hydrogen adsorption at 77 K, especially on the samples with high metal loading of, such as in my case, 20 wt%. On the one hand, surface area-dependent physisorption dominated the hydrogen adsorption capacity at 77 K; On the other hand, high metal loading and calcinations resulted in the significant drop of surface area and micropore volume of the sample, thus much less hydrogen adsorption capacities from physisorption were obtained. For example, the surface area decreased from 887 to 553 m^2/g and micropore volume decreased from 0.335 to 0.174 cm^3/g, respectively, after 20 wt% of Ni was loaded onto the NaY support. Under these circumstances, difference between undoped NaY and reduced NiNaY was not suitable for the estimation of spiltover hydrogen.

The estimation of spiltover hydrogen can be done by expressing the experimentally observed hydrogen storage capacity of nickel-doped zeolite as a linear combination of the hydrogen storage capacities of nickel nanoparticles, zeolite support and that due to the spillover. Hydrogen adsorption capacities on undoped NaY, calcined NiNaY and reduced NiNaY can be expressed as the following equations:

Combined hydrogen adsorption on reduced NiNaY :

$$H_R = H_{Ni} + H_{NaY\text{-}R} + H_s$$

Combined hydrogen adsorption on calcined NiNaY : $H_C = H_{NaY\text{-}C}$ (assumes that the hydrogen adsorption on NiO particles is negligible)

Hydrogen adsorption on NaY support : $H = H_{NaY}$

H_{NaY} represents the hydrogen adsorption capacity on undoped NaY support, $H_{NaY\text{-}C}$ and $H_{NaY\text{-}R}$ represent the hydrogen adsorption capacities on NaY support of calcined and reduced NiNaY composite, H_{Ni} represents hydrogen adsorption capacity on nickel nanoparticles of reduced NiNaY. H_s represents amount of spiltover hydrogen.

For the hydrogen adsorption on reduced samples with low metal loadings, the surface area and micropore volume dropped negligibly compared with those of undoped NaY, so $H_{NaY\text{-}R}$ was very close to H_{NaY}. Thus it was very reasonable to use the difference between hydrogen capacities of undoped NaY and the reduced NiNaY to calculate the $H:M_S$ ratio. However, for the hydrogen adsorption on reduced samples with high metal loading, the surface area and micropore volume dropped significantly compared with those of undoped NaY, so H_{NaY} was much larger than $H_{NaY\text{-}R}$. Thus the difference between hydrogen capacities of undoped NaY and the reduced NiNaY cannot be used to calculate the $H:M_S$ ratio. For instance, the differences between hydrogen adsorption capacities of undoped NaY and the reduced 20%NiNaY were negative values at 77 K and both pressures (−0.02 wt% at 0.1 MPa, −0.45 wt% at 10 MPa). Considering calcined NiNaY and reduced NiNaY composites possessed very close surface areas and pore volumes (see Table 1), hydrogen adsorption on calcined NiNaY composites can be assumed equal to the hydrogen adsorption on the NaY support of reduced NiNaY composites ($H_{NaY\text{-}R} = H_{NaY\text{-}C} = H_C$). The difference between hydrogen adsorption capacities of calcined and reduced NiNaY composites thus were from hydrogen adsorbed on nickel particles and spiltover hydrogen. This difference amount was used to calculate the $H:M_S$ ratio, which can be used to assess hydrogen spillover effect.

The $H:M_S$ ratios for the reduced NiNaY composites under various adsorption conditions were calculated and listed in Table 4. All $H:M_S$ ratios under various conditions were bigger than unity

indicating that the spillover was occurring on the reduced NaY composites. The increased pressure and decreased temperature significantly increased the H:M_S ratios suggesting that the spillover effect has been greatly enhanced under these conditions. Hydrogen spillover is generally thought to be proportional to the square root of pressure, however, this common assumption is based on Langmuir's model and not directly linked to experimental data. Rather, hydrogen spillover as a surface phenomenon should relate directly to surface concentration gradients and only indirectly to hydrogen pressure [5]. The surface hydrogen concentration increased at low temperature or high pressure and the corresponding H:M_S ratios also increased significantly, which suggested improved hydrogen spillover effect.

4. Conclusions

Hydrogen adsorption capacities of reduced NiNaY composites were significantly enhanced under various temperatures and pressures. The enhancement effect of hydrogen adsorption on the reduced composites at room temperature was determined by hydrogen adsorption on available nickel sites which were characterized by the active nickel surface areas. However, the optimized hydrogen adsorption enhancement effect on the composite at 77 K was achieved by a combination of suitable active nickel surface area and active support area. Hydrogen to surface nickel ratios under various conditions were bigger than unity indicating that the spillover was occurring on the reduced NaY composites. The result is encouraging and optimized metal–adsorbent composites are promising media achieving higher hydrogen adsorption capacity at suitable conditions.

References

[1] J.A. Schwarz, Metal Assisted Carbon Cold Storage of Hydrogen, 5 Jan, 1988, US Patent 4716736, Syracuse University, Syracuse, New York.
[2] J.S. Noh, R.K. Agarwal, J.A. Schwarz, Int. J. Hydrogen Energy 12 (10) (1987) 693–700.
[3] W.C. Conner, J.L. Falconer, Chem. Rev. 95 (3) (1995) 759–788.
[4] F.H. Yang, R.T. Yang, Carbon 40 (3) (2002) 437–444.
[5] A.D. Lueking, R.T. Yang, Appl. Catal. A 265 (2) (2004) 259–268.
[6] A.J. Lachawiec, G.S. Qi, R.T. Yang, Langmuir 21 (24) (2005) 11418–11424.
[7] Y.W. Li, R.T. Yang, J. Am. Chem. Soc. 128 (3) (2006) 726–727.
[8] Y.W. Li, R.T. Yang, J. Phys. Chem. B 110 (34) (2006) 17175–17181.
[9] Y.W. Li, R.T. Yang, J. Am. Chem. Soc. 128 (25) (2006) 8136–8137.
[10] R.T. Yang, Y.H. Wang, J. Am. Chem. Soc. 131 (12) (2009) 4224–4226.
[11] Y.W. Li, F.H. Yang, R.T. Yang, J. Phys. Chem. C 111 (8) (2007) 3405–3411.
[12] Y.W. Li, R.T. Yang, J. Phys. Chem. C 111 (29) (2007) 11086–11094.
[13] Y.W. Li, R.T. Yang, AIChE J. 54 (1) (2008) 269–279.
[14] L.F. Wang, R.T. Yang, Energy Environ. Sci. 1 (2) (2008) 268–279.
[15] C.-H. Chen, C.-C. Huang, Micropor. Mesopor. Mater. 109 (1–3) (2008) 549–559.
[16] C.I. Contescu, C.M. Brown, Y. Liu, V.V. Bhat, N.C. Gallego, J. Phys. Chem. C 113 (14) (2009) 5886–5890.
[17] B.-J. Kim, Y.-S. Lee, S.-J. Park, Int. J. Hydrogen Energy 33 (15) (2008) 4112–4115.
[18] Y.-Y. Liu, J.-L. Zeng, J. Zhang, F. Xu, L.-X. Sun, Int. J. Hydrogen Energy 32 (16) (2007) 4005–4010.
[19] D. Scarano, S. Bordiga, C. Lamberti, G. Ricchiardi, S. Bertarione, G. Spoto, Appl. Catal. A 307 (1) (2006) 3–12.
[20] E. Yoo, L. Gao, T. Komatsu, N. Yagai, K. Arai, T. Yamazaki, K. Matsuishi, T. Matsumoto, J. Nakamura, J. Phys. Chem. B 108 (49) (2004) 18903–18907.
[21] M. Zielinski, R. Wojcieszak, S. Monteverdi, M. Mercy, M.M. Bettahar, Int. J. Hydrogen Energy 32 (8) (2007) 1024–1032.
[22] L. Zubizarreta, J.A. Menéndez, J.J. Pis, A. Arenillas, Int. J. Hydrogen Energy 34 (7) (2009) 3070–3076.
[23] R. Campesi, F. Cuevas, R. Gadiou, E. Leroy, M. Hirscher, C. Vix-Guterl, M. Latroche, Carbon 46 (2) (2008) 206–214.
[24] L.F. D'Elia, I. González, K. Saavedra, V. Gottberg, Int. J. Hydrogen Energy 34 (4) (2009) 1958–1964.
[25] B. Chen, J.G. Goodwin, J. Catal. 148 (1) (1994) 409–412.
[26] D.H. Everett, Manual of Symbols and Terminology for Physicochemical Quantities and Units, Butterworths, London, 1971.
[27] P. Benard, R. Chahine, Scr. Mater. 56 (10) (2007) 803–808.
[28] A.J. Lachawiec, R.T. Yang, Langmuir 24 (12) (2008) 6159–6165.
[29] A.J. Lachawiec, R.T. Yang, J. Phys. Chem. C 113 (31) (2009) 13933–13939.
[30] D.G. Mustard, C.H. Bartholomew, J. Catal. 67 (1981) 186–206.
[31] J.E. Benson, M. Boudart, J. Catal. 4 (6) (1965) 704–710.
[32] M. Boudart, J. Mol. Catal. 30 (1–2) (1985) 27–38.
[33] B.C. Gates, Chem. Rev. 95 (1995) 511–522.